Supporting Information

Se-hollow porous carbon composite for high-performance rechargeable K-Se batteries

Xianglong Huang [a,b], Wei Wang[a], Jianhua Deng[a,b], Wei Gao [a,b], Dingyu Liu [a,b], Qianru Ma[b], Maowen Xu [a,b,*]

[a] School of Materials and Energy, Southwest University, Chongqing 400715, P. R. China.

[b] Chongqing Key Laboratory for Advanced Materials and Technologies of Clean Energies, Chongqing 400715, P.R. China..

*Corresponding author. Tel/Fax: +86-023-68254732; E-mail: xumaowen@swu.edu.cn.

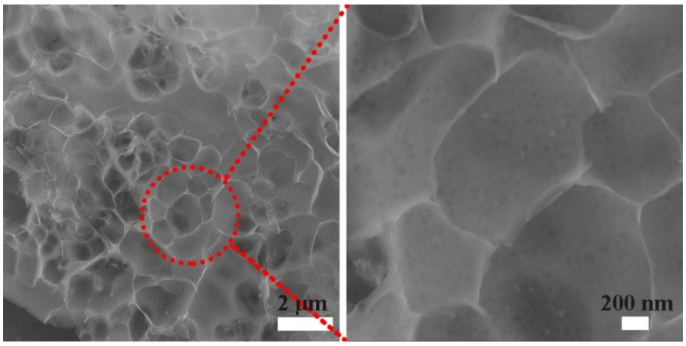

Figure. S1. FESEM images of surface of HPC matrix.

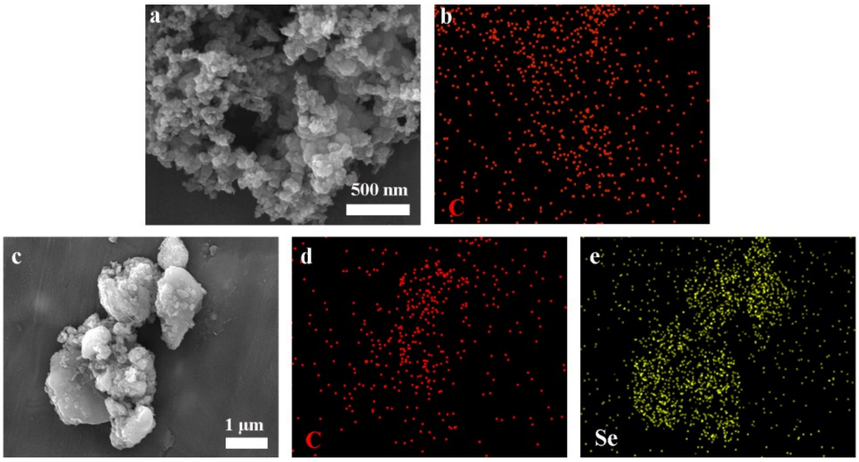

Figure S2. (a-b) FESEM image and elemental mapping of AB; (c-e) FESEM image and elemental mappings of the Se/AB mixture.

Table S1

Comparison of the porosity between this work and other K-Se studies.

Matrix material	Specific surface area (m^2 g^{-1})	Pore size distribution (nm)	Retained specific surface area (m^2 g^{-1})	Se content (wt%)	Ref.
c-PAN	not available	not available	not available	39	[16]
NOPC-CNT	877.2	0.8~4.0	12.6	60	[17]
MPDC	511	0.8~4.5	13	53	[21]
HPC	**416**	**1.0~4.0**	**48**	**42**	**This work**

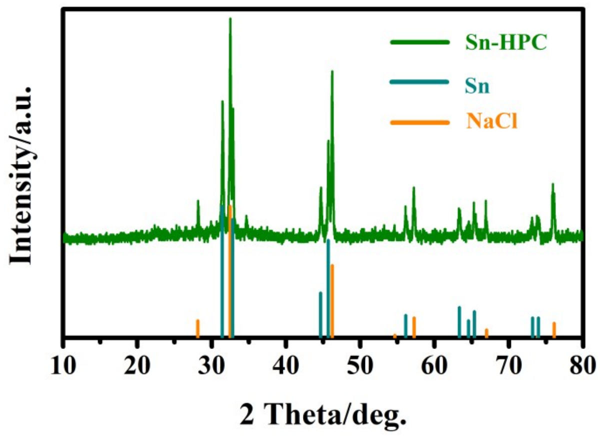

Figure. S3. XRD pattern of Sn-HPC complex with NaCl.

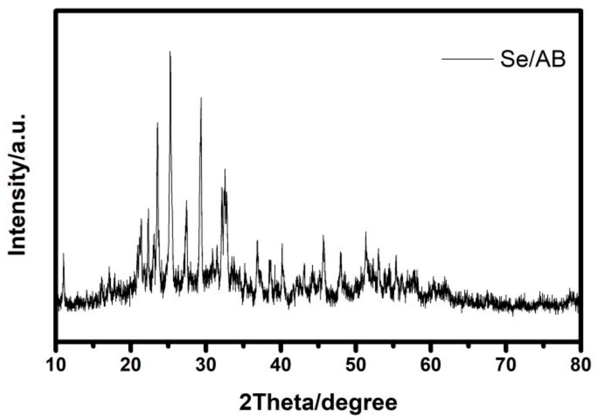

Figure S4. XRD patterns of Se/AB mixture.

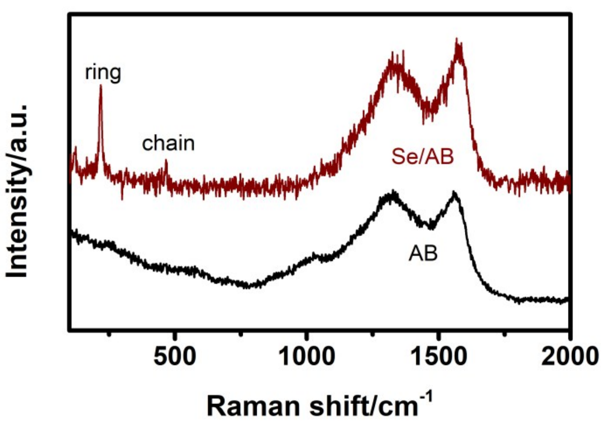

Figure S5. Raman spectra of Se/AB mixture.

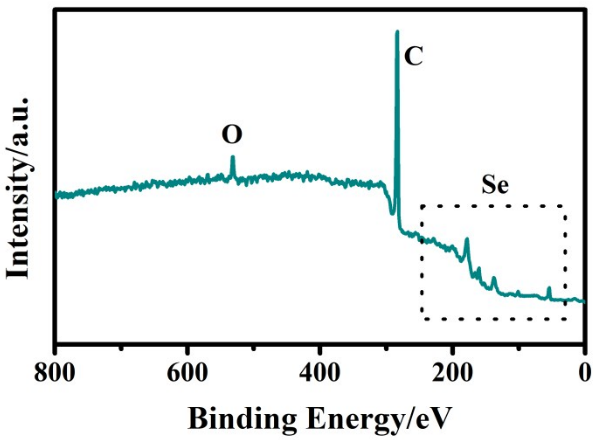

Figure. S6. XPS spectra of survey for the Se-HPC composite.

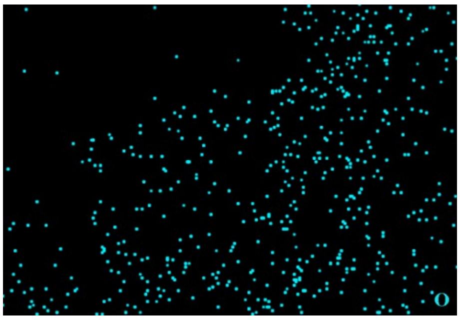

Figure. S7. Elemental mapping of O for Se-HPC composite.

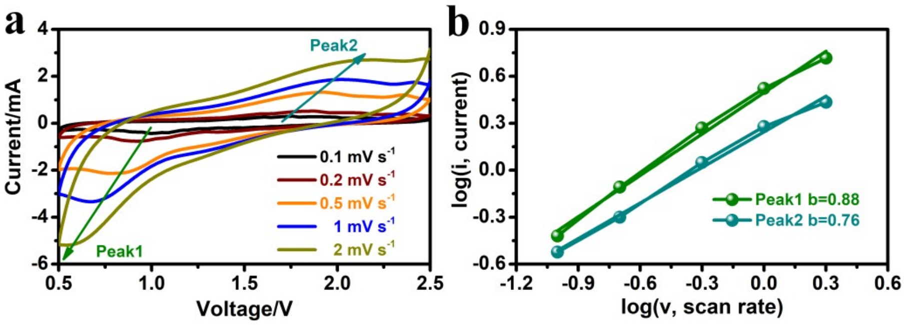

Figure S8. (a) CV curves of the Se-HPC composite at various rates; (b) The linear fitting plots of the log10-transformed peak currents versus scan rates.

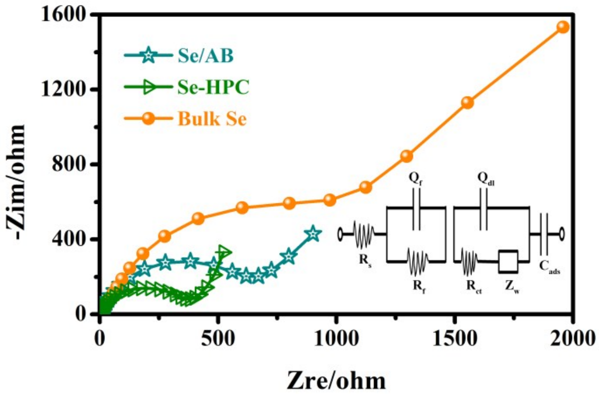

Figure S9. Nyquist plots of the battery with the fresh bulk Se, Se/AB and Se-HPC composite before cycling.

Table S2

Comparison of Rct.

Sample	Rct/ Ω
Se	931.6
Se/AB	525.1
Se-HPC	333.7

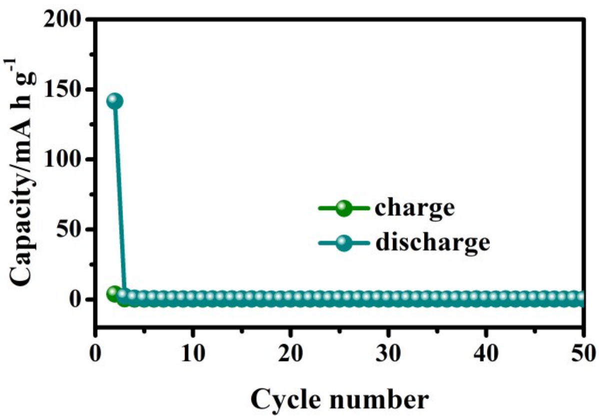

Figure. S10. Cycling performance of the Se/AB mixture at 0.2 C.

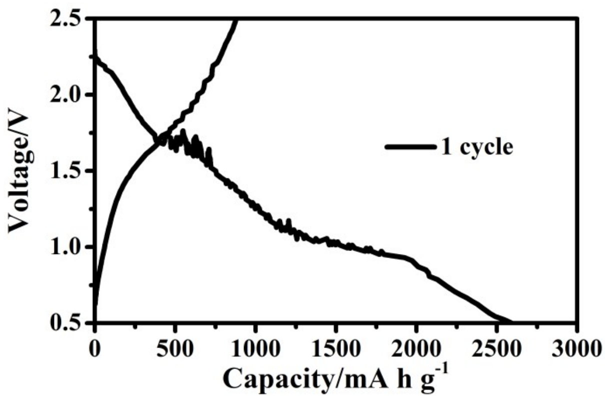

Figure. S11. Discharge-charge profile of Se-HPC composite at the first cycle at 0.2 C.

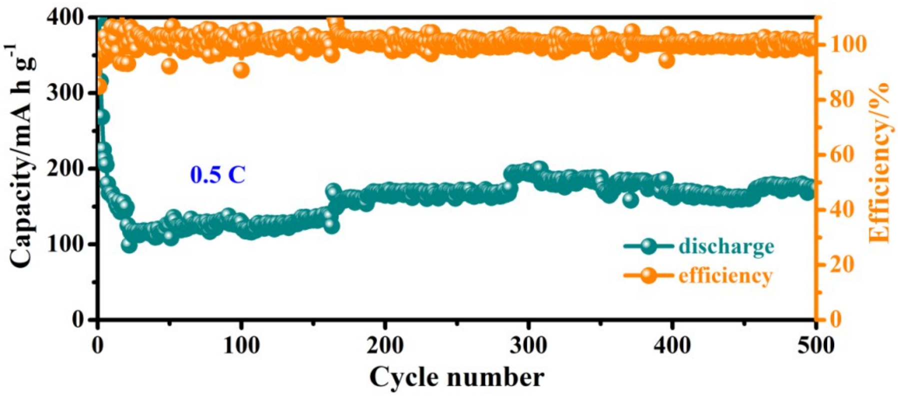

Figure. S12. Prolonged cycling performance of cathode electrode at the current density of 0.5 C.

Table S3

Comparison of electrochemical performance of this work with previous publications for K-Se batteries.

Cathode material	Se content (wt %)	Current density (mA g^{-1})	Reversible capacity (mA h g^{-1})	Cycle number	Ref.
c-PAN-Se composite	39	135	652	100	[16]
Se@NOPC-CNT composite	60	100	585	700	[17]
Se/MPDC composite	53	135	327	100	[21]
Se-HPC composite	**42**	**135**	**872**	**100**	**This work**

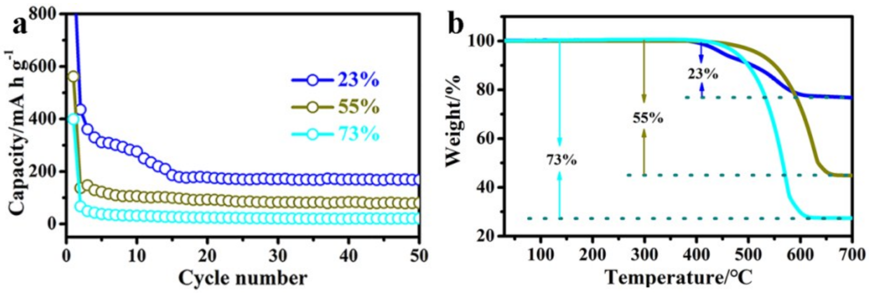

Figure S13. (a) Discharge capacity of the Se-HPC composite with different contents at 0.2 C; (b) TGA curves of the Se-HPC composite with different contents.

Figure S14. The mechanism diagram of Se content impact on electrochemical performance.

The explanation is as the following:

Firstly, volumetric expansion of active materials can occupy the whole hollow sphere to lead to the lack of transport pathway for K^+ ions for the composite with high Se content. Moreover, the excess of Se may result in the problem that part of Se adheres to carbon matrix surfaces to cause terrible capacity delivery [1]. Secondly, there exists a lot of residual volume in the Se-HPC composite with low Se content of 23 % and a large amount of electrolyte can swarm into the residual space. As electrochemical behaviors occur, some or much active materials can escape from the physical confinement of HPC matrix to pose great continuous loss of Se and diffusion into electrolyte [2]. Therefore, the composite with low or high Se content both exhibits a relatively worse electrochemical performance. On the contrary, the HPC matrix host confines the active materials very well as well as creating transport pathway for K+ ions for the composite with an ideal Se content [3].

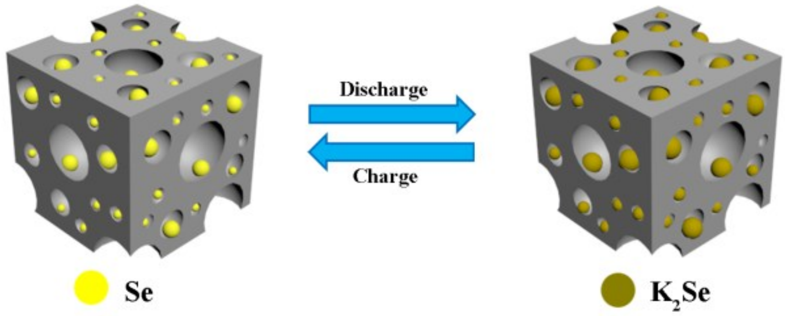

Figure. S15. Schematic illustration of reaction mechanism of the cathode materials.

References

[1] Q.J. Xu, T. Liu, Y. Li, L.Y. Hu, C.L. Dai, Y. Zhang, Y. Li, D.Y. Liu, M.W. Xu, ACS Appl. Mater. Interfaces 2017, 9, 41339-41346.

[2] B.B Yuan, X.Z.n Sun, L.C. Zeng, Y. Yu, Q.S. Wang, Small 2017, 1703252

[3] J.J. Zhang, L. Fan, Y.C. Zhu, Y.H. Xu, J.W. Liang, D.H. Wei, Y.T. Qian, Nanoscale, 2014, 6, 12952-12957.